PERGAMON

Materials Science in Semiconductor Processing 1 (1998) 99–106

MATERIALS SCIENCE IN SEMICONDUCTOR PROCESSING

The effect of TEM sample thickness on nucleation and growth and dissolution of {311} defects in Si^+ implanted Si

Jing-Hong Li[a,*], Mark E. Law[b], Craig Jasper[c], Kevin S. Jones[a]

[a]*SWAMP Center, Department of Materials Science and Engineering, 525 Engineering Building, University of Florida, P.O. Box 116130, Gainesville, FL 32611-6130, USA*

[b]*Department of Electrical and Computer Engineering, 525 Engineering Building, University of Florida, P.O. Box 116130, Gainesville, FL 32611-6130, USA*

[c]*ACT, Motorola Inc., 2200 W. Broadway, Mesa, AZ 85202, USA*

Abstract

The effect of sample thickness on the nucleation, growth and dissolution of {311} defects in non-amorphizing 100 keV, 2×10^{14} cm^{-2} Si^+ implanted Si has been investigated by plan-view transmission electron microscopy (PTEM) and cross-section TEM (XTEM). The samples were annealed at 800°C for times between 5 and 30 min. Results from samples annealed prior to TEM sample preparation were compared with samples annealed after thinning for TEM. The observed region in the TEM in both cases was 4000 Å thick. TEM showed both the {311} extended defects and sub-threshold dislocation loops formed upon annealing. The depth distribution of these defects is centered around the ion damage profile. Quantitative TEM was used to measure the trapped interstitial concentration. The total interstitial concentration trapped in {311} defects and loops after annealing at 800°C for 5 min was determined to be $\sim 1 \times 10^{14} \pm 1 \times 10^{13}$ cm^{-2} for the thick samples and $\sim 0.9 \times 10^{14} \pm 1 \times 10^{13}$ cm^{-2} for the thin samples. The rate constant for {311} dissolution was determined from quantitative TEM to be 420 s for both the thick and thin samples. The existence of the second surface in the thin samples may affect the nucleation process slightly, but the existence of the second surface 2000 Å below the implant layer has no measurable effect on the coarsening and dissolution of {311} defects and the evolution of the sub-threshold loops. This implies that the surface must be less than 2000 Å from the implant layer to affect the interstitial evolution. © 1998 Elsevier Science Ltd. All rights reserved.

Keywords: Sample thickness; {311} defects; dislocation loops; defect evolution; annealing kinetics; TEM

1. Introduction

It is well known that both {311} defects and dislocation loops can form upon annealing of ion implanted Si and that upon dissolution the {311} defects are a source of transient enhanced diffusion (TED) of dopants [1–5]. Because of the drive toward ever decreasing transistor sizes, there is a need to better understand the mechanisms of how these defects form and evolve and the role that the surface plays in this evolution. Quantitative transmission electron microscopy (TEM) has been developed as a method to study the evolution of these defects. In order to study the role of the surface on the evolution of the defects this study exploits the fact that the process of fabricating a TEM sample results in the formation of a second surface in close proximity to the damage layer. The effect of the second surface on the evolution of the

* Corresponding author. Tel.: +1-352-392-8463; Fax: +1-352-392-8381; E-mail: jli@mail.mse.ufl.edu.

1369-8001/98/$ - see front matter © 1998 Elsevier Science Ltd. All rights reserved.
PII: S1369-8001(98)00013-4

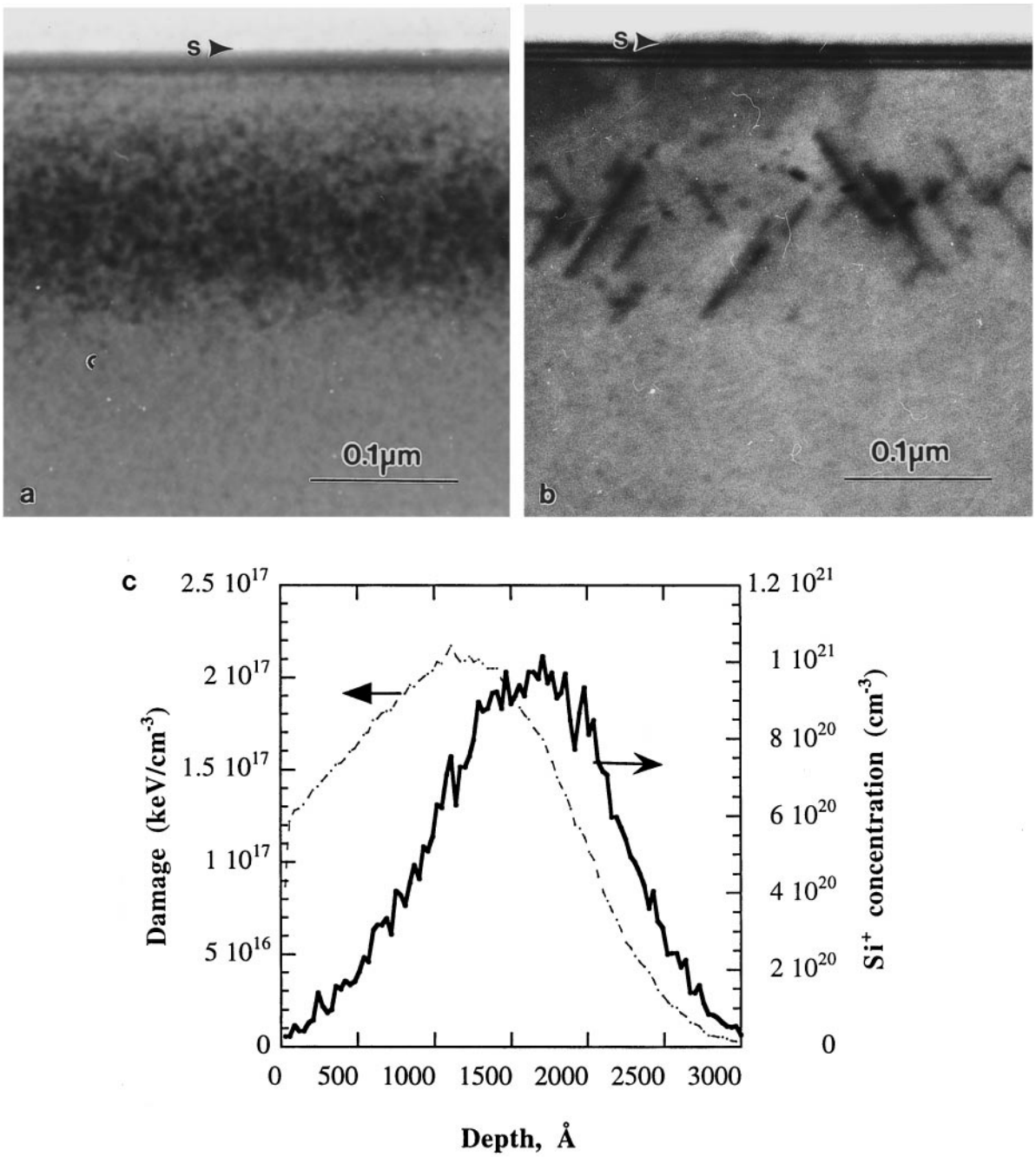

Fig. 1. Cross-sectional TEM images of 100 keV 2×10^{14} cm^{-2} Si^+ implanted Si: (a) as-implanted, (b) after 800°C for 20 min anneal and (c) TRIM simulation.

implant damage can be studied by comparing samples annealed in a bulk state with samples annealed after TEM sample preparation. It is found that the presence of this second surface does not significantly affect the {311} or dislocation loop evolution for non-amorphizing Si implants.

2. Experimental

Czochralski-grown (001) Si was implanted with Si^+ with a dose of 2×10^{14} cm^{-2} and an energy of 100 keV at a temperature of 20°C, a dose rate of 4 $\mu A/cm^2$ and tilt of 5°. Two types of samples were annealed

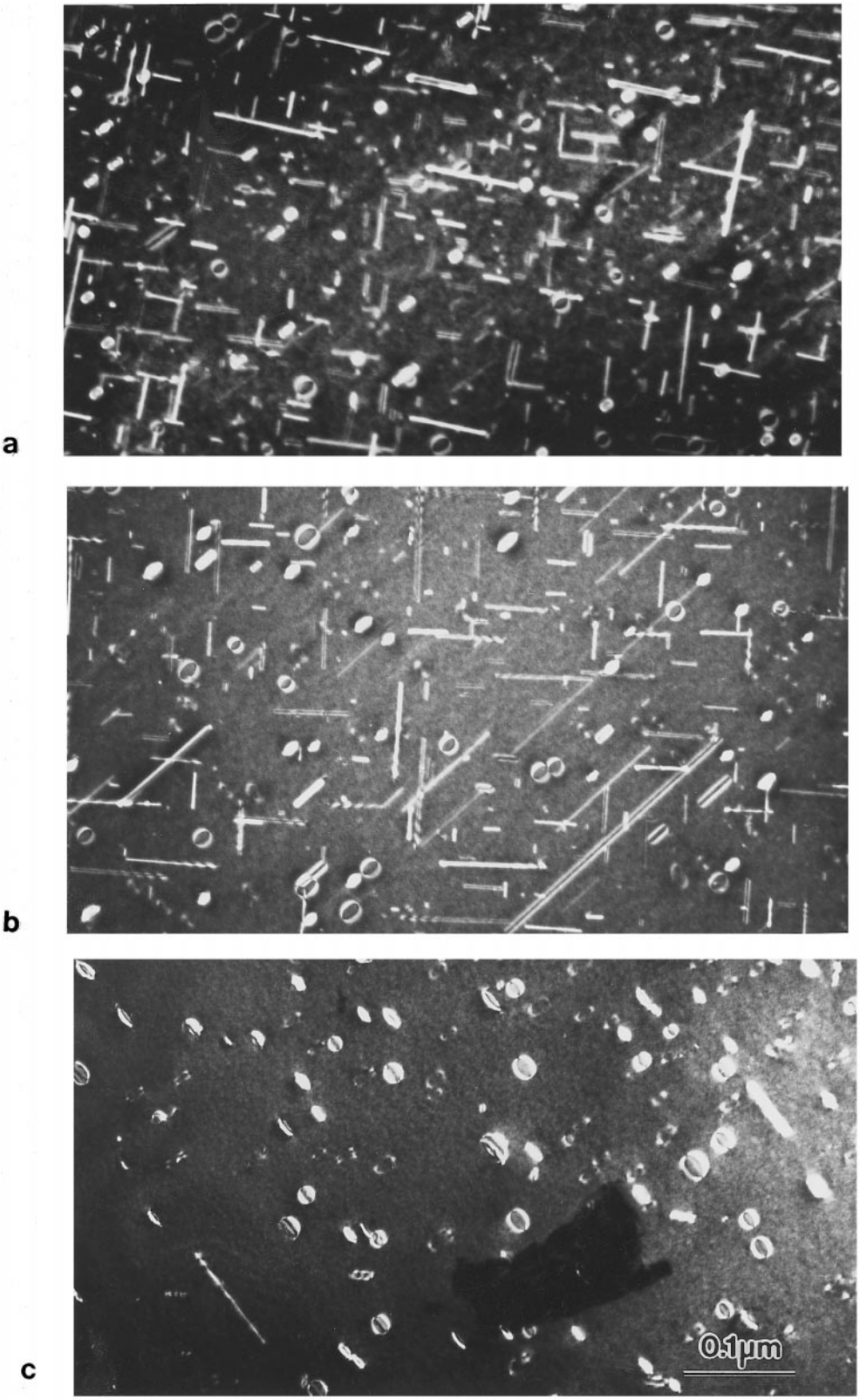

Fig. 2(a–c).

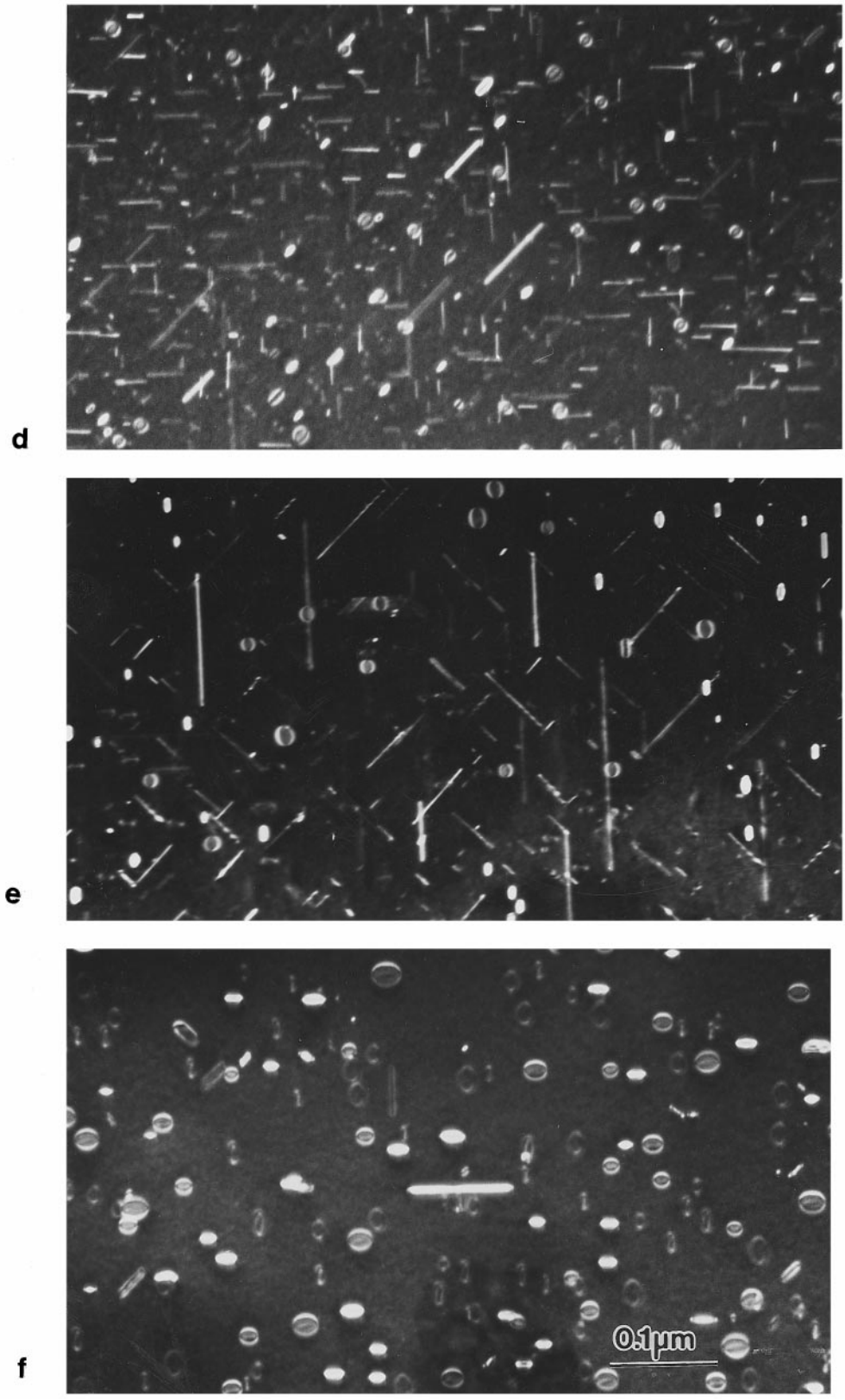

Fig. 2. Plan-view TEM images of 100 keV 2×10^{14} cm^{-2} Si^{+} implanted Si for thick (400 μm) samples annealed at 800°C: (a) 10 min, (b) 20 min and (c) 30 min and thin (0.4 μm) samples annealed at 800°C: (d) 10 min, (e) 20 min and (f) 30 min.

simultaneously at 800°C for different times from 5 to 30 min in furnace with a flowing N_2 ambient. One type of sample was a normal wafer with a thickness of 400 μm which was annealed prior to thinning (thick) and the other type was thinned for TEM observation prior to annealing (thin). TEM sample preparation was done by first mechanically grinding down to about 100 μm, then etching a hole from the back side using $HF:HNO_3$ solution. Both the thick samples and the thin samples were annealed at the same time. After annealing, the thick samples were prepared into plan-view and cross-section TEM samples. TEM observations were performed in a JEOL 200CX TEM microscope operating at 200 kV. Plan-view TEM micrographs were taken using g_{220} weak beam dark field imaging conditions. The thickness of the thinned sample was determined by the fringe spacing at $s = 0$ and by convergent-beam electron diffraction. Interstitial concentrations were measured by TEM using the method previously discussed [6].

3. Results and discussion

Fig. 1 shows the cross-section TEM images of 400 μm thick Si^+ implanted Si both as implanted (a) and after annealing at 800°C for 20 min (b). Fig. 1c shows the TRIM simulation for the 100 keV and 2×10^{14} cm^{-2} Si^+ implant. From Fig. 1a, it can be seen that there was no amorphous layer formed and the depth of the visible damage zone extends from 450 Å to a depth of about ~1700. After annealing at 800°C for 20 min, the defect layer of {311} defects and dislocation loops similarly extended from 450 to 1700 Å. The extent of the damage was also compared with the ion and damage profile determined by TRIM (95) [7]. At a value of 70% of the peak concentration the damage distribution extended from 400 to 1700 Å while the ion distribution extends from 1200 to 2200 Å. It was noted many years ago that the ion dose matches the trapped interstitial concentration in loops quantitatively [1] and this became the now highly referenced 'plus one' model [8]. Despite the fact that the implanted ion dose predicts the concentration of interstitials remarkable well, the damage profile does the best job of predicting the {311} depth distribution. It is suggested that this is because after Frenkel pair recombination the probability is much greater that the remaining interstitial per incident ion will reside in the region where the interstitials population before recombination was the greatest, i.e. around the damage profile.

Fig. 2a–c shows PTEM images of the defect evolution for the samples which were 400 μm thick during annealing at 800°C for 10, 20 and 30 min, respectively and Fig. 2d–f also shows the PTEM images of the regions that were 4000 Å thick during annealing at 800°C for 10, 20 and 30 min, respectively. It can be seen that {311} defects formed after initial 10 min anneal, then increased in size and decreased in defect density over the 30 min anneal for both the 400 μm thick samples and the 4000 Å thick regions. Sub-threshold loops formed in both types of samples. From the images it can be seen that the {311} dislocation size and loop size in the both samples is very similar.

Fig. 3 shows the results of quantifying the interstitial concentrations (cm^{-2}) trapped in {311} dislocations and loops for the thick samples and thin samples after 800°C anneal for various times. Fig. 3 reveals that the 400 μm thick samples and the 4000 Å thick samples had almost the same initial (5 min anneal) interstitial concentration (8×10^{13} cm^{-2} versus 6.3×10^{13} cm^{-2}, respectively). For both the thick and thin samples, the interstitial's concentration trapped in the {311} defects decreased as the annealing time increases while the interstitial concentration trapped in the loops increased as the annealing time increases. The total interstitial concentration trapped in the {311} defects and sub-threshold loops for the thick and thin samples was roughly at $\sim 1 \times 10^{14}$ cm^{-2} and 9×10^{13} cm^{-2} after 5 min anneal at 800°C, respectively. After annealing at 800°C for 30 min the {311} defects were gone and the total trapped interstitial content in the defects (loops only) decreased to around 5×10^{13} cm^{-2}. Thus there was a net release of interstitials from the visible defects of around 5×10^{13} cm^{-2}. The increase in interstitials in the loops was the result of increases in both the size and number of loop. The nucleation of loops from {311} defects will be discussed in a second paper [9].

Fig. 4 shows: (a) the {311} defect and loop density and (b) the variation of average loop diameters for the 400 μm thick samples and the 4000 Å thick samples after annealing. Again, the 400 μm thick samples and the 4000 Å thick samples show similar dissolution behaviour. Upon annealing the {311} defect and loop densities decreased. Fig. 4b shows that upon annealing between 5 min and 30 min the average loop diameter increased, from ~137 and ~120 to ~300 and ~295 Å for thick and thin samples, respectively. But, the {311} density drops more sharply than the loop density since the {311}'s are dissolving whereas the loops are undergoing a growth and coarsening process.

From the results above, it is clearly seen that the existence of a second surface ~2000 Å below the implant damage has no significant effect on the formation and dissolution of {311} defects and sub-threshold dislocation loops. The 'plus' value [10] is defined as the ratio of the trapped interstitials in the defects to the implant dose. Eaglesham et al. reported a plus value of 1.4 for 40 keV and 5×10^{13} cm^{-2} Si^+ implants [5]. For this experiment if one extrapolates the dissolution curves in Fig. 3 to $t = 0$, the estimated

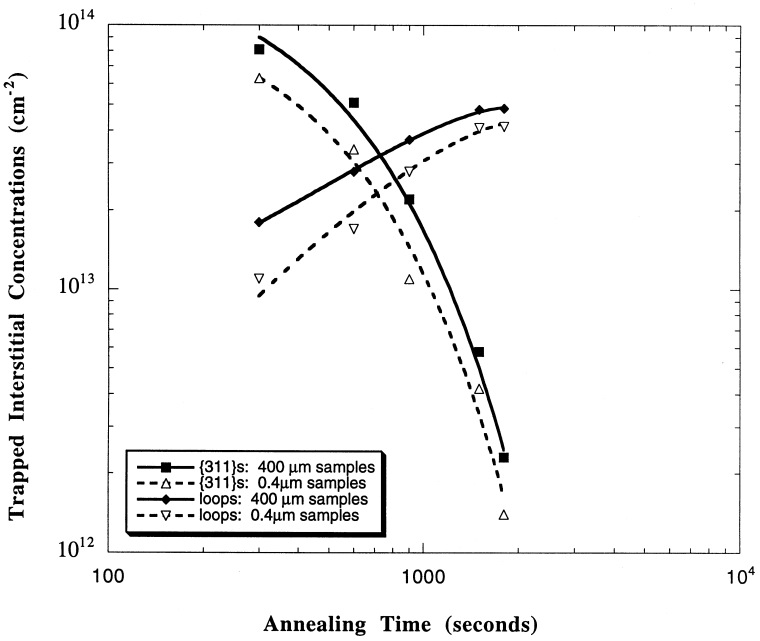

Fig. 3. Trapped interstitial concentration in {311} defects and dislocation loops for thick and thin samples after annealing at 800°C for various times.

plus value is between +0.9 and +0.7 for the thick and thin samples, respectively. The slightly lower plus value is presumably the result of either differences in the starting material (float zone in their case and Czochralski in this experiment) or differences in quantification methods.

In addition to the plus value, the rate constant for {311} dissolution can be determined from Fig. 3. Because the decay shows an exponential dependence on time, the Si interstitial concentration, $[Si]_{int}$, could be expressed as

$$[Si]_{int} = C_o \exp(-t/\tau), \quad (1)$$

where C_o is the 'plus' value at $t = 0$ and the τ is the characteristic decay rate constant at the measured temperature (800°C for this experiment). The decay rate constant shows an Arrhenius temperature dependence [5] and can therefore be expressed as

$$\tau_{311} = \tau_o \exp(\Delta E/kT), \quad (2)$$

where τ_o is the pre-exponential factor, ΔE is the activation energy, k is Boltzmann's constant and T is the temperature. From Fig. 3, τ_{311} was determined to be 420 s for both the thick and thin samples. Stolk et al. [11] showed the rate constant to have an activation energy of 3.6 eV. From their plot, the decay time τ_{311} for {311} dissolution for a 40 keV 5×10^{13} cm^{-2} Si^+ implant at 800°C was estimated to be about 70 s. This is a considerably smaller decay time, i.e. the {331} defects dissolve much faster for their experiment. There are several potential reasons for the difference in {311} decay times. First, there could have been an error in the calibration of the furnace temperature. If this were the case, the temperature would have had to be 750°C not 800°C to explain this difference based on Stolk's Arrhenius relationship and their decay curves [11]. The furnace temperature in this experiment was calibrated several times using different thermocouples imbedded in a test wafer and the temperature is believed to be accurate to ±5°C. The different counting techniques would presumably introduce a plus value shift but not a rate constant shift as long as a single method is used for all times. There was an energy and dose difference in the implant conditions from 40 keV 5×10^{13} cm^{-2} to 100 keV 2×10^{14} cm^{-2}. The lower implant energy brought the {311}'s closer to the surface that could accelerate their dissolution. However, it has recently been shown also from the same group [12] that decreasing the Si^+ implant energy to only 5 keV (1×10^{14} cm^{-2}) results in a time constant of $\tau_{311} = 440$ s at 750°C which corresponds to a time constant of $\tau_{311} \sim 70$ sec at 800°C assuming a 3.6 eV activation energy again. This is exactly the same rate constant as they measured for the 40 keV 5×10^{13} cm^{-2} Si^+ implant. Thus, if the change in projected range from 40 keV to 5 keV does not affect the {311} dissolution rate, then the decrease in the depth from 100 to 40 keV also is not likely to have a major effect. It has been proposed by Agarwal et al. [12] that when the peak interstitial concentration

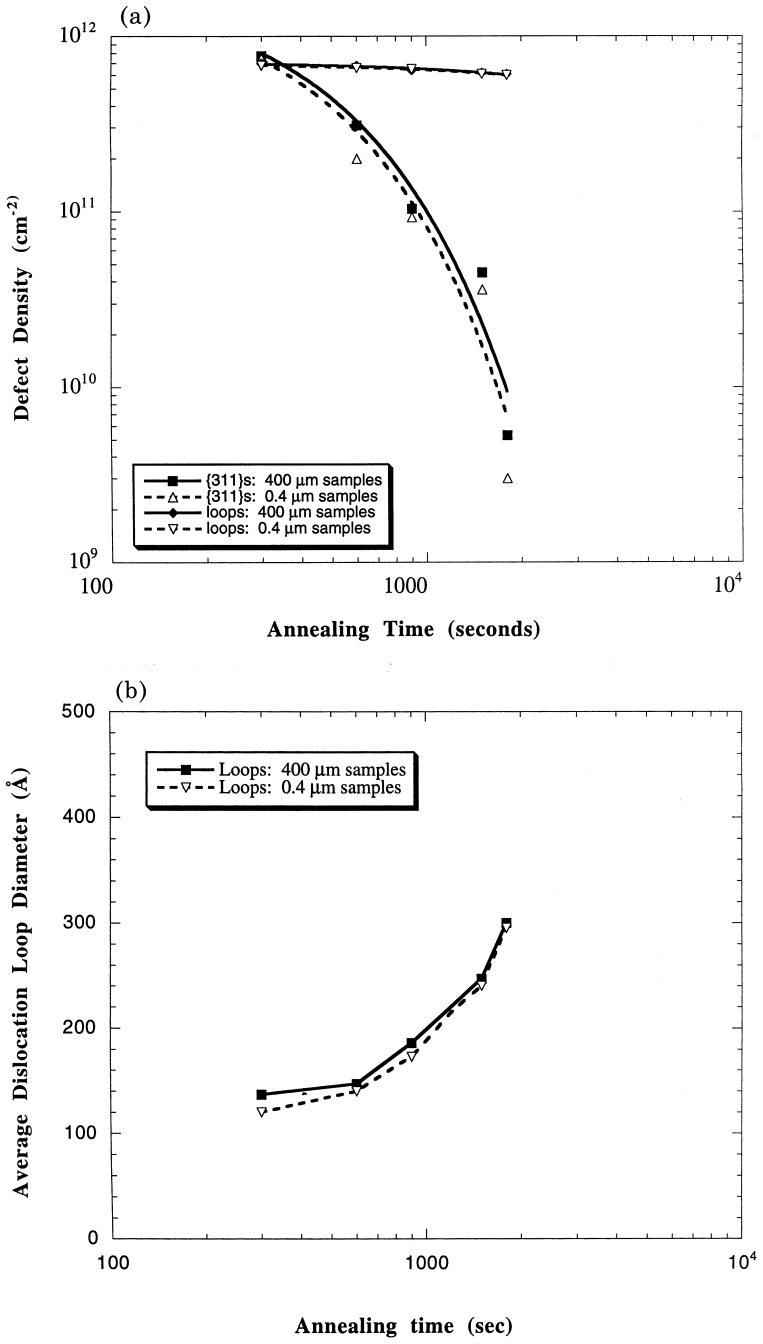

Fig. 4. (a) Density of {311} defects and dislocation loops and (b) average dislocation loop diameter for thick and thin samples after annealing at 800°C for various times.

exceeds 1%, zig-zag defects form. They have shown that such zig-zag {311} defects can be very stable for 5 keV 3×10^{14} cm^{-2} Si^+ implanted Si, exhibiting a dissolution time constant of $\tau_{311} = 2860$ s at 750°C. Again assuming a 3.6 eV activation energy, this corresponds to a value of $\tau_{311} = 440$ s at 800°C. This is very similar to our value of $\tau_{311} = 420$ s at 800°C. In addition, the peak concentration of interstitials was estimated by TRIM, Fig. 1c, to be about 2%. This implies that zig-zag {311} defects should be present for the implant used in this sample however no zigzag defects were observed in the TEM. Further work look-

ing for these defects is continuing. Another factor which could contribute to the slow time constant for these higher dose samples is the formation of dislocation loops. The 100 keV 2×10^{14} cm^{-2} sample was above the stable dislocation loop formation threshold [1]. This raises the issue of the role of the presence of dislocation loops on the {311} decay process. The presence of the dislocation loops may have a stabilizing effect on the {311} decay process. In addition, since {311} defects appear to be the source of the dislocation loops [8], their annealing kinetics are inextricably intertwined and further experiments are necessary to sort out this relationship.

4. Conclusions

The effect of sample thickness on the nucleation, growth and dissolution of {311} defects in non-amorphizing 100 keV, 2×10^{14} cm^{-2} Si^{+} implanted Si has been investigated by plan-view TEM (PTEM) and cross-section TEM (XTEM). The samples were annealed at 800°C for times between 5 and 30 min. Results from samples annealed prior to TEM sample preparation were compared with samples annealed after thinning for TEM (4000 Å). TEM showed that both {311} extended defects and the sub-threshold loops formed upon annealing and these defects formed at the peak of the damage profile not the ion profile. From corresponding quantitative TEM interstitial measurements, the total interstitials concentration trapped in the {311} defects and loops was determined to be $+0.5$ of the dose independent of sample thickness during annealing. A time constant of 420 s for {311} decay was found for both thick and thin samples. The existence of the second surface 2000 Å below the implanted layer in the thin samples may affect the {311} nucleation process slightly, but it had no measurable effect on the coarsening and dissolution of {311} defects and the evolution of the subthreshold loops. The presence of the dislocation loops may slow the {311} dissolution rate.

Acknowledgements

The authors would like to thank Allen Hoover at Motorola for the Si^{+} implant and the SEMATECH for financial supporting this work. The authors also like to thank Dr. Viswanath Krishnamoorthy for his valuable discussion and Kathryn Moller and Michael Wright for their help in TEM sample preparation.

References

[1] Jones KS, Prussin S, Weber ER. Appl Phys A 1988;45:1.
[2] Schretelkamp RJ, Custer JS, Liefting JR, Lu WX, Saris FW. Mat Sci Rep 1991;6:275.
[3] Liefting JR, Schretelkamp RJ, Vanhellemount J, Vandervorst W, Maex K, Custer JS, Saris FW. Appl Phys Lett 1993;63:1134.
[4] Stolk PA, Gossmann H-J, Eaglesham DJ, Jacobson DC, Ratherty CJ, Giller GH, Jaraiz M, Poate JM, Luftman HS, Haynes TE. J Appl Phys 1997;81(9):6031.
[5] Eaglesham DJ, Stock PA, Gossmann H-J, Haynes TE, Poate JM. Nucl Instr Meth Phys Res B 1995;106:191.
[6] Jones KS, Liu J, Zhang L, Krishnamoorthy V, Dehoff RT. Nucl Instr Meth Phys Res B 1995;106:227.
[7] TRIM. New York: Pergmon Press, 1995.
[8] Giles MD. J Electrochem Soc 1991;138:1160.
[9] Li J.H., Jones K.S., unpublished.
[10] Jones K.S., Ph.D. thesis, University of California at Berkeley, 1989.
[11] Stolk P.A., Gossmann H.-J., Eaglesham D.J., Jacobson D.C., Luftman H.S., Poate J.M. Mat Res Soc Symp Proc 1995:354.
[12] Agarwal A, Haynes TE, Eaglesham DJ, Gossmann H-J, Jacobson DC, Erokhin YuE. Appl Phys Lett 1997;70:3332.